ATLAS NOTE

ATLAS-CONF-2014-056

27th September 2014

Measurement of spin correlation in top–antitop quark events and search for top squark pair production in proton–proton collisions at $\sqrt{s}$=8 TeV using the ATLAS detector

The ATLAS Collaboration

Abstract

A measurement of spin correlation in $t\bar{t}$ production is presented using data collected with the ATLAS detector at the Large Hadron Collider (LHC) in proton–proton collisions at a center-of-mass energy of 8 TeV, corresponding to an integrated luminosity of 20.3 fb^{-1}. The correlation between the top and antitop quark spins is extracted from dilepton $t\bar{t}$ events by using the difference in azimuthal angle between the two charged leptons in the laboratory frame. In the helicity basis the measured degree of correlation corresponds to $A_{\text{helicity}} = 0.38 \pm 0.04$, in agreement with the Standard Model prediction. A search is performed for pair production of top squarks with masses close to the top quark mass decaying to predominantly right-handed top quarks and a light neutralino, the lightest supersymmetric particle. Top squarks with masses between the top quark mass and 191 GeV are excluded at the 95% confidence level.

ATLAS-CONF-2014-056
30 September 2014

1 Introduction

Detailed studies of the properties of the top quark are of great interest. They provide important precision tests of the predictions of the Standard Model (SM) and allow searches for physics beyond the SM (BSM). In particular, the measurement of the orientation of the spin of top quarks produced in pairs is sensitive to many BSM theories [1–7]. For example, the measured spin correlation would deviate from the SM value if $t\bar{t}$ pairs were produced via the exchange of a virtual heavy scalar Higgs boson [8], if the top quark decay occured via a charged Higgs boson and a b-quark ($t \to H^+ b$) [9–15], or if pairs of supersymmetric (SUSY) top squarks were produced [16].

The lifetime of the top quark is much shorter than the timescale for strong interactions, such that the top quark decays before hadronization [17–23]. Therefore the spin of the top quark at production is transferred to its decay products and can be measured directly via their angular distributions [19]. While the polarization of t and $\bar{t}$ quarks in a hadronically produced $t\bar{t}$ sample is predicted to be very small, the orientation of their spins is predicted to be correlated [19, 24–43].

The strength of the correlation of the spin of top and antitop quarks in $t\bar{t}$ events has been studied previously by the CDF and D0 collaborations in proton–anti-proton scattering at 1.98 TeV [44–47] and by the ATLAS and CMS collaborations in proton-proton scattering at 7 TeV [48–50].

In this Note the first measurement of $t\bar{t}$ spin correlation at proton–proton collisions at a center-of-mass energy of 8 TeV is presented. At a collision energy of 8 TeV, a slightly larger spin correlation is expected compared to 7 TeV [43]. [1] Dilepton final states are analyzed, because the spin-analyzing power of the charged leptons from top and antitop quark decays is effectively 100%. The azimuthal angle $\Delta\phi$ between charged leptons is very sensitive to $t\bar{t}$ spin correlation [41], and is also well measured by the ATLAS detector.

First, the measurement of $\Delta\phi$ is used to extract the spin correlation strength A_{helicity}, which is a measure of the fraction of events where the top quark and top antiquark spins are parallel minus the fraction of events where they are anti-parallel with respect to a spin quantization axis. This axis is chosen to be the helicity basis, using the direction of flight of the top quark in the center-of-mass frame of the $t\bar{t}$ system. Secondly, in a study of a specific model that leads to zero spin correlation, a search for SUSY top squark pair production is performed.

At the LHC, the SUSY partners of the top quark, the top squarks, could be produced in pairs. Models with light top squarks are particularly attractive since they provide a solution to the hierarchy problem. In such models, the mass $m_{\tilde{t}_1}$ of the lighter top squark mass eigenstate $\tilde{t}_1$ could be close to the mass of the top quark m_t [51, 52]. If the lightest SUSY particle, the neutralino $\tilde{\chi}_1^0$ (or gravitino), is light and the top squark mass is only slightly larger than the top quark mass,[2] two body decays $\tilde{t}_1 \to t\tilde{\chi}_1^0$ in which the momentum of $\tilde{\chi}_1^0$ is very small can predominate [16]. In SUSY models where R-parity is conserved, such as the Minimal Supersymmetric Standard Model (MSSM) [53–57], this could lead to $t\bar{t}\tilde{\chi}_1^0\tilde{\chi}_1^0$ intermediate states, appearing like SM $t\bar{t}$ production with additional missing transverse momentum carried away by the escaping neutralinos, making traditional searches exploiting kinematic differences as presented in Refs. [58–64] very difficult. Apart from an increase of the measured $t\bar{t}$ cross section as analyzed in Ref. [65], as top squarks have spin-0, $\tilde{t}_1\bar{\tilde{t}}_1$ events can be distinguished from SM $t\bar{t}$ events by measuring angular correlations sensitive to spin correlation, as analyzed in this Note.

A description of the ATLAS detector can be found elsewhere [66].

[1] ATLAS uses a right-handed coordinate system, with its origin at the nominal interaction point in the center of the detector. The z-axis points along the beam direction, the x-axis from the interaction point to the center of the LHC ring, and the y-axis upwards. In the transverse plane, cylindrical coordinates (r, ϕ) are used, where ϕ is the azimuthal angle around the beam direction. The pseudorapidity η is defined via the polar angle θ as $\eta = -\ln\tan(\theta/2)$.

[2] The masses of all other SUSY particles are assumed to be large.

2 Sample composition and modeling

This analysis uses proton–proton collision data with a center-of-mass energy of $\sqrt{s} = 8$ TeV, corresponding to an integrated luminosity of 20.3 fb^{-1}.

Monte Carlo (MC) simulation samples are used to evaluate the contributions, and shapes of distributions of kinematic variables, for signal $t\bar{t}$ events and background processes not evaluated from complementary data samples. All MC samples are processed with the GEANT4 [67] simulation of the ATLAS detector [68] and are passed through the same analysis chain as data. The simulation includes multiple proton–proton interactions per bunch crossing (pile-up). Events are weighted such that the distribution of the average number of interactions per bunch crossing matches that observed in data.

Samples of $t\bar{t}$ events with SM spin correlation and without spin correlation are generated using MC@NLO v4.06 [69, 70] interfaced to Herwig v6.520 [71] for shower simulation and hadronization. For the no-spin-correlation sample the parton shower simulation performs isotropic decays of the top quarks as opposed to using the full matrix element as used for the generation of the SM spin correlation sample. For both samples, the CT10 PDF set [72] is used, the production cross section is normalized to the cross section calculated in next-to-next-to-leading-order (NNLO) Quantum Chromodynamics (QCD) including corrections in next-to-next-to-leading-log (NNLL) [73–85], and the top quark mass is set to 172.5 GeV. The production of a $t\bar{t}$ pair in association with a Z or W boson is simulated using Madgraph [86] interfaced to Pythia v6.426 [87] normalized to the next-to-leading-order (NLO) QCD cross sections [88].

Backgrounds to same-flavor dilepton $t\bar{t}$ production arise from the Drell–Yan Z/γ^*+jets production process with the Z/γ^* boson decaying into e^+e^- or $\mu^+\mu^-$. In the $e^\pm\mu^\mp$ channel, one of the main backgrounds is due to Z/γ^*+jets production with decays $Z/\gamma^* \to \tau^+\tau^-$, followed by leptonic decays of the τ leptons. Drell–Yan events are generated using the Alpgen v2.13 [88] generator including leading-order (LO) matrix elements with up to five additional partons. The CTEQ6L1 PDF set [89] is used, and the cross section is normalized to the NNLO prediction [90]. Parton showering and fragmentation are modeled by Herwig, and the underlying event is simulated by Jimmy [91]. To avoid double counting of partonic configurations generated by both the matrix-element calculation and the parton-shower evolution, a parton–jet matching scheme ("MLM matching") [92] is employed. Events using explicit $Z/\gamma^* + c\bar{c}$ and $Z/\gamma^* + b\bar{b}$ matrix elements with decays $Z/\gamma^* \to e^+e^-, \mu^+\mu^-, \tau^+\tau^-$ are generated in addition. The yields of dielectron and dimuon Drell–Yan events predicted by the MC simulation are compared to the data in Z/γ^*+jets-dominated control regions. Correction factors are derived and applied to the predicted yields in the signal region, to account for the difference between the simulation prediction and data.

Single top quark background arises from associated Wt production, when both the W boson emerging from the top quark and the W boson from the hard interaction decay leptonically. This contribution is modeled with Powheg-Box r2129 [93–96] interfaced with Pythia using the CT10 PDF set [72] and normalized to the approximate NNLO QCD theoretical cross section [97]. Single top Zt and WZt production is generated by Madgraph interfaced with Pythia.

The diboson (WW, WZ, ZZ) backgrounds are modeled using Sherpa v1.4.1 [98] and are normalized to the theoretical calculation at NLO QCD [99].

The background arising from the misidentified and non-prompt leptons (collectively referred to as "fake leptons") is determined from a combination of MC simulation of W+jets events using Sherpa, single top quark events via t-channel exchange using MC@NLO+Herwig, $t\bar{t}$ events with single lepton final states using MC@NLO+Herwig, and data using a technique known as the matrix method [100, 101].

Top squark pair production samples are simulated for top squark masses in the range 175–230 GeV and neutralino masses in the range 1 GeV$< m_{\tilde{\chi}_1^0} < m_{\tilde{t}_1} - m_t$ using the Herwig++ v2.6.1 [102] generator with the CTEQ6L1 PDFs [89] normalized to the NLO cross-sections including next-to-leading log (NLL) corrections [103]. The top squarks are assumed to decay exclusively via $\tilde{t}_1 \to t\tilde{\chi}_1^0$. The corresponding mixing matrices for the top squarks and for the neutralinos are chosen such that the top quark produced in the $\tilde{t}_1 \to t\tilde{\chi}_1^0$ decay has a right-handed polarization in 95% of the decays. It has been found that the shape of the $\Delta\phi$ distribution is unaffected by changing the handedness. Therefore, the scenario of left-handed polarized top quarks from top squark decay is not investigated further.

3 Event selection

Candidate events are selected in the dilepton topology. Channels with τ leptons are not explicitly considered, but reconstructed leptons can arise from leptonic τ decays and are included in the simulated samples. The analysis requires events selected online by inclusive single-lepton triggers (e or μ). Electron candidates are reconstructed from an isolated electromagnetic calorimeter energy deposit matched to an ID track of charged particles and passing medium identification requirements [104]. Muon candidates were reconstructed by combining matching tracks reconstructed in both the ID and MS [105]. Jets are reconstructed from clusters of adjacent calorimeter cells [66, 106] using the anti-k_t algorithm [107–109] with a radius parameter $R = 0.4$. Jets originating from b-quarks were identified ('tagged') using a multivariate discriminant making use of the long lifetime, high decay multiplicity, hard fragmentation and high mass of B hadrons [110, 111]. The missing transverse momentum ($E_{\mathrm{T}}^{\mathrm{miss}}$) is reconstructed as the magnitude of a vector sum of all calorimeter cell energies associated with topological clusters [112]. The following kinematic requirements are made:

- Electron candidates are required to have $p_{\mathrm{T}} > 25$ GeV and $|\eta| < 2.47$, excluding electrons from the transition region between the barrel and end-cap calorimeters defined by $1.37 < |\eta| < 1.52$. Muon candidates are required to have $p_{\mathrm{T}} > 25$ GeV and $|\eta| < 2.5$. Events must have exactly two oppositely-charged lepton candidates (e^+e^-, $\mu^+\mu^-$, $e^\pm\mu^\mp$).

- Events must have at least two jets (after having removed jets that match an electron candidate) with $p_{\mathrm{T}} > 25$ GeV and $|\eta| < 2.5$. At least one jet must be identified as a b-jet using a requirement in the multivariate discriminant corresponding to a 70% b-tagging efficiency.

- Events in the e^+e^- and $\mu^+\mu^-$ channels must satisfy $E_{\mathrm{T}}^{\mathrm{miss}} > 30$ GeV to suppress backgrounds from Z/γ^*+jets and W+jets events.

- Events in the e^+e^- and $\mu^+\mu^-$ channels are required to have $m_{\ell\ell} > 15$ GeV (where ℓ indicates e or μ) to ensure compatibility with the simulated backgrounds and remove contributions from Υ and J/ψ production. In addition, $m_{\ell\ell}$ must differ by at least 10 GeV from the Z-boson mass ($m_Z = 91$ GeV) to further suppress the Z/γ^*+jets background.

- For the $e^\pm\mu^\mp$ channel, no $E_{\mathrm{T}}^{\mathrm{miss}}$ or $m_{\ell\ell}$ requirements are applied. In this case, the remaining background from $Z/\gamma^*(\to \tau\tau)$+jets production is further suppressed by requiring that the scalar sum of the p_{T} of all selected jets and leptons is greater than 130 GeV.

The expected numbers of $t\bar{t}$ signal and background events are compared to data in Table 1. The expected yield for top squark pair production with a top squark mass of 180 GeV and a neutralino mass of 1 GeV is also shown. The number of observed events in each channel is: 13343 for the e^+e^- channel,

Process	Yield
$t\bar{t}$	54000^{+3400}_{-3600}
Z/γ^*+jets	2800 ± 300
tV (single top)	2600 ± 180
$t\bar{t}V$	80 ± 11
WW, WZ, ZZ	180 ± 65
Fake Leptons	780 ± 780
Total non-$t\bar{t}$	6400 ± 860
Expected (E)	60000^{+3500}_{-3700}
Observed (O)	60424
$\tilde{t}_1\bar{\tilde{t}}_1$	7100 ± 1100
($m_{\tilde{t}_1} = 180$ GeV, $m_{\tilde{\chi}^0_1} = 1$ GeV)	

Table 1: Observed dilepton yield in data and the expected SUSY and $t\bar{t}$ signals and background contributions. Systematic uncertainties due to theoretical cross sections and systematic uncertainties evaluated for data-driven backgrounds are included in the uncertainties.

14084 for the $\mu^+\mu^-$ channel and 32997 for the $e^\pm\mu^\mp$ channel, which is larger than the sum of the other two yields due to the looser selection criteria.

4 Measurement procedure

Figure 1 shows the reconstructed $\Delta\phi$ distribution for the sum of the three dilepton channels in data. A binned log-likelihood fit is used to extract the spin correlation from the $\Delta\phi$ distribution in data. This is done defining the coefficient f_{SM}, which gives a measure of agreement with the spin correlation expected in the SM. The fit includes a linear superposition of the $\Delta\phi$ distribution from SM $t\bar{t}$ MC simulation with coefficient f_{SM}, and from the uncorrelated $t\bar{t}$ MC simulation with coefficient $(1 - f_{\mathrm{SM}})$. The e^+e^-, $\mu^+\mu^-$ and $e^\pm\mu^\mp$ channels are fitted simultaneously with a common value of f_{SM}, leaving the $t\bar{t}$ normalization free with a fixed background normalization. The $t\bar{t}$ normalization obtained by the fit is in agreement with the theoretical prediction of the production cross section [78]. Negative values of f_{SM} correspond to an anti-correlation of the top and antitop quark spins. A value of $f_{\mathrm{SM}} = 0$ implies that the spins are uncorrelated and values of $f_{\mathrm{SM}} > 1$ indicate a larger strength of the $t\bar{t}$ spin correlation than predicted by the SM. The extraction of f_{SM} using the fitting procedure has been verified over a wide range of possible values, $-1 \leq f_{\mathrm{SM}} \leq 2$, using MC-simulated pseudo-experiments with full detector modeling.

5 Systematic uncertainties

Systematic uncertainties are evaluated by applying the fit procedure to pseudo-experiments created from simulated samples modified to reflect the systematic variations. The fit of f_{SM} is repeated to determine the effect of each systematic uncertainty using the nominal templates. The difference between the means of Gaussian fits to the results from many pseudo-experiments using nominal and modified pseudo-data is taken as the systematic uncertainty on f_{SM} [113].

The different sources of uncertainties are estimated in the same way as in Ref. [49] with the following exceptions: since this analysis employs b-tagging, the associated uncertainty is estimated varying

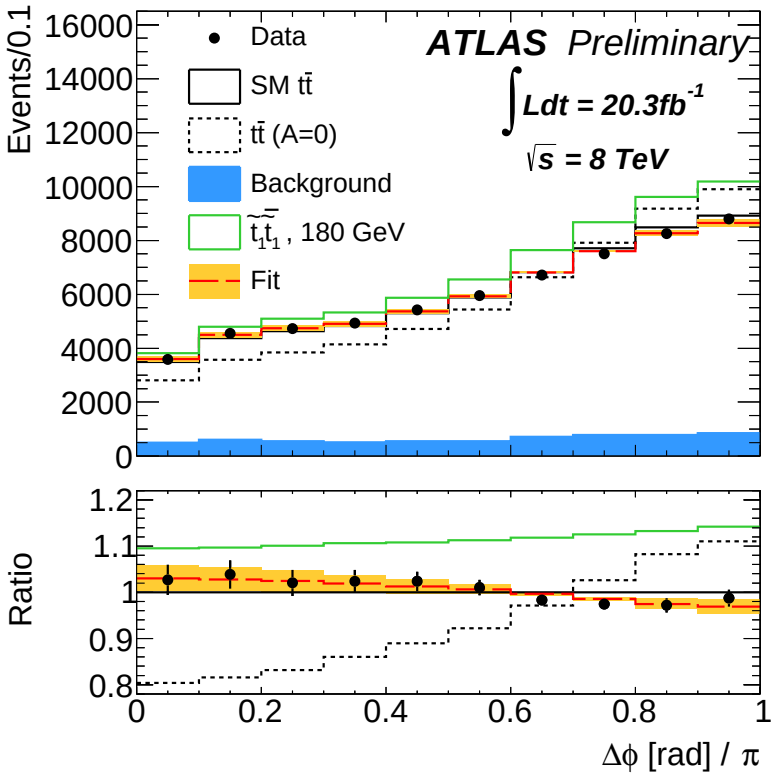

Figure 1: Reconstructed $\Delta\phi$ distribution for the sum of the three dilepton channels. The prediction for background (blue histogram) plus SM $t\bar{t}$ production (solid black histogram) and background plus $t\bar{t}$ prediction with no spin correlation (dashed black histogram) is compared to the data and to the result of the fit to the data (red dashed histogram) with the orange band representing the total systematic uncertainty on $f_{\rm SM}$. Both the SM $t\bar{t}$ and the no spin correlation $t\bar{t}$ predictions are normalized to the NNLO+NNLL cross section [78]. The prediction for $\tilde{t}_1\bar{\tilde{t}}_1$ production ($m_{\tilde{t}_1}$ = 180 GeV and $m_{\tilde{\chi}_1^0}$ = 1 GeV) normalized to the NLO+NLL cross section [103] plus SM $t\bar{t}$ production plus background is also shown (solid green histogram). The lower plot shows those distributions (except for background only) divided by the SM $t\bar{t}$ plus background prediction.

the relative normalizations of simulated b-jet, c-jet and light-jet samples. The uncertainty due the choice of the generator is determined by comparing the default $t\bar{t}$ sample generated by MC@NLO interfaced with Herwig to an alternative $t\bar{t}$ sample generated with the Powheg-Box generator interfaced with Pythia. The uncertainty due to the parton shower and hadronization model is determined by comparing two $t\bar{t}$ samples generated by Alpgen, one interfaced with Pythia and the other one interfaced with Herwig. The uncertainty on the amount of initial- and final-state radiation (ISR/FSR) in the simulated $t\bar{t}$ sample is assessed by comparing Alpgen, showered with Pythia, with varied amounts of initial- and final-state radiation. As in Ref. [49], the size of the variation is compatible with the recent measurements of additional jet activity in $t\bar{t}$ events [114]. The Wt normalization is varied within the theoretical uncertainties of the cross section calculation [97], and the sensitivity to the interference between Wt production and $t\bar{t}$ production at NLO is studied by comparing the predictions of Powheg-Box with the diagram-removal (baseline) and diagram-subtraction schemes [96,115]. As in Ref. [49], the uncertainty due to the top quark mass is not included in the systematic uncertainties, but would have no significant

Source of uncertainty	Δf_{SM}
Detector modeling	
Lepton reconstruction	±0.01
Jet energy scale	±0.02
Jet reconstruction	±0.01
E_T^{miss}	< 0.01
Fake leptons	< 0.01
b-tagging	< 0.01
Signal and background modeling	
Renormalization/factorization scale	±0.05
MC generator	±0.03
Parton shower and fragmentation	±0.06
ISR/FSR	±0.06
Underlying event	±0.04
Color Reconnection	±0.01
PDF Uncertainty	±0.05
Background	±0.01
MC statistics	±0.04
Total systematic uncertainty	±0.13
Data statistics	±0.05

Table 2: Summary of systematic uncertainties on f_{SM} in the combined dilepton final state.

impact on the results.

The size of the systematic uncertainties in terms of Δf_{SM} are listed in Table 2. The total systematic uncertainty is calculated by combining all systematic uncertainties in quadrature.

6 Spin correlation strength

The measured value of f_{SM} for the combined fit is found to be 1.20 ± 0.05 (stat) ± 0.13 (syst). This agrees with previous results from ATLAS using data at a center-of-mass energy of 7 TeV [48, 49] and agrees with the SM prediction to within 2 standard deviations. An indirect extraction of $A_{helicity}$ can be achieved under the assumption that the $t\bar{t}$ sample is composed of top quark pairs as predicted by the SM, but with varying spin correlation. In that case, a change in the fraction f_{SM} will lead to a linear change of $A_{helicity}$ (see also Ref. [49]), and a value of the spin correlation strength in the helicity basis $A_{helicity}$ at a center-of-mass energy of 8 TeV is obtained by applying the measured value of f_{SM} as a multiplicative factor to the SM prediction of $A_{helicity}^{SM} = 0.318 \pm 0.005$ [43]. This yields a measured value of $A_{helicity} = 0.38 \pm 0.04$.

7 Spin correlation in top squark pair production

The measurement of the variable $\Delta\phi$ is also used to search for top squark pair production with $\tilde{t}_1 \to t\tilde{\chi}_1^0$ decays. The present analysis is sensitive to both changes in the yield and changes in the shape of the $\Delta\phi$ distribution caused by potential $\tilde{t}_1\bar{\tilde{t}}_1$ admixture with the SM $t\bar{t}$ sample. An example is shown in

Fig. 1 where the effect of $\tilde{t}_1\bar{\tilde{t}}_1$ production in addition to SM $t\bar{t}$ production and backgrounds is compared to data. No evidence for $\tilde{t}_1\bar{\tilde{t}}_1$ production has been found.

Limits are set on the top squark pair production cross section by fitting each bin of the $\Delta\phi$ distribution to the difference between the data and the SM prediction, varying the top squark signal strength μ. In contrast to the measurement of f_{SM} where the $t\bar{t}$ cross section is varied in the fit, here the $t\bar{t}$ cross section is fixed to its SM value [78], and the uncertainty, composed of factorisation and renormalization scale variation, top quark mass uncertainty, PDF uncertainty and uncertainty in the measurement of the beam energy, is introduced as an additional systematic uncertainty. All other sources of systematic uncertainties are identical to the measurement of f_{SM}. All shape-dependent modeling uncertainties on the SUSY signal are found to be negligible. The limits are determined using a profile likelihood ratio in the asymptotic limit [116], using nuisance parameters to account for the theoretical and experimental uncertainties.

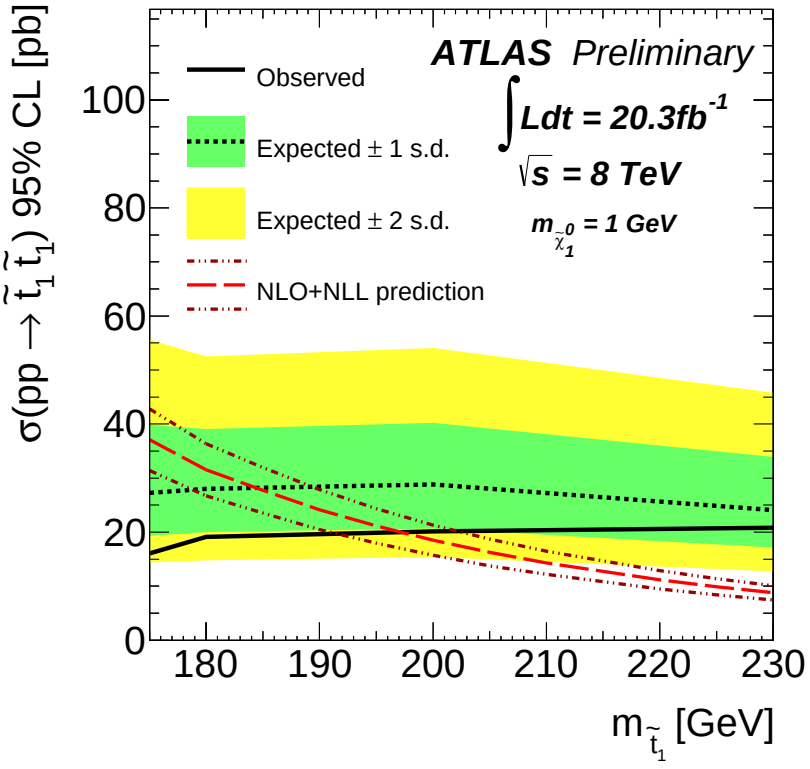

Figure 2: Expected and observed limits at 95% CL on the top squark pair production cross section as a function of $m_{\tilde{t}_1}$, for pair produced top squarks $\tilde{t}_1$ decaying with 100% branching ratio via $\tilde{t}_1 \to t\tilde{\chi}_1^0$ to predominantly right-handed top quarks, assuming $m_{\tilde{\chi}_1^0} = 1$ GeV. The black dotted line shows the expected limit with ±1 (green) and ±2 (green+yellow) standard deviation contours, taking into account all uncertainties. The red dashed line shows the theoretical cross section with uncertainties. The solid black line gives the observed limit.

The observed and expected limits on the top squark pair production cross section at the 95% confidence level (CL) are extracted using the CLs prescription [117] and are shown in Fig. 2. Adopting the convention of reducing the estimated SUSY production cross section by one standard deviation of its theoretical uncertainty (15%, coming from PDFs and QCD scale uncertainties [118]), top squark

masses between the top mass threshold and 191 GeV are excluded, assuming 100% branching ratio for $\tilde{t}_1 \to t\tilde{\chi}_1^0$ and $m_{\tilde{\chi}_1^0} = 1$ GeV. The expected limit is 178 GeV. In the presented range of $m_{\tilde{t}_1}$, within the allowed phase space, varying the neutralino mass does not affect the limits by more than a few percent. If the $t\bar{t}$ cross section normalization was arbitrary and not fixed to its theory uncertainty, the expected cross section limit would increase by approximately 30%. If, on the other hand, the shape information of $\Delta\phi$ were not used in the fit, the expected cross section limit would increase by 30-40%. This is in approximate agreement with the expected limit on the identical SUSY scenario derived from a measurement of the $t\bar{t}$ cross section at a center-of-mass energy of 8 TeV as presented in [65]. Therefore, the constraints presented here extend those previous limits to larger excluded top squark masses. The limits also extend constraints from analyses exploring kinematic distributions, such as presented in Ref. [62] where top squark masses larger than 210 GeV are excluded.

8 Conclusion

In conclusion, the first measurement of $t\bar{t}$ spin correlation in proton–proton scattering at a center-of-mass energy of 8 TeV has been presented using 20.3 fb^{-1} of ATLAS data in the dilepton decay topology. A template fit is performed to the $\Delta\phi$ distribution and the measured value of f_{SM} =1.20 ± 0.05 (stat) ± 0.13 (syst) is consistent with the SM prediction. The results have been used to search for pair-produced supersymmetric top squarks decaying to top quarks and light neutralinos. Assuming 100% branching ratio for the decay $\tilde{t}_1 \to t\tilde{\chi}_1^0$, and the production of predominantly right-handed top quarks, top squark masses between the top quark mass and 191 GeV are excluded at 95% CL, which is an improvement over previous constraints.

References

[1] R. Frederix and F. Maltoni, JHEP **0901**, 047 (2009).

[2] M. Arai, N. Okada and K. Smolek, Phys. Rev. D **79**, 074019 (2009).

[3] G. L. Kane, G. A. Ladinsky and C. P. Yuan, Phys. Rev. D **45**, 124 (1992).

[4] K. Cheung, Phys. Rev. D **55**, 4430 (1997).

[5] J. Y. Liu, Z. G. Si and C. X. Yue, Phys. Rev. D **81**, 015011 (2010).

[6] J. S. Lee, Y. Peters, A. Pilaftsis and C. Schwanenberger, Eur. Phys. J. C **66**, 261 (2010).

[7] M. S. Carena, S. Heinemeyer, C. E. M. Wagner and G. Weiglein, Eur. Phys. J. C **26**, 601 (2003).

[8] W. Bernreuther, M. Flesch and P. Haberl, Phys. Rev. D **58**, 114031 (1998).

[9] T. Aaltonen *et al.* [CDF Collaboration], Phys. Rev. Lett. **103**, 101803 (2009).

[10] V. M. Abazov *et al.* [D0 Collaboration], Phys. Rev. D **80**, 071102 (2009).

[11] V. M. Abazov *et al.* [D0 Collaboration], Phys. Lett. B **682**, 278 (2009).

[12] ATLAS Collaboration, JHEP **1206**, 039 (2012).

[13] CMS Collaboration, JHEP **1207**, 143 (2012).

[14] ATLAS Collaboration, JHEP **1303**, 076 (2013).

[15] ATLAS Collaboration, Eur. Phys. J. C **73**, 2465 (2013).

[16] Z. Han, A. Katz, D. Krohn and M. Reece, JHEP **1208**, 083 (2012).

[17] I. Bigi *et al.*, Phys. Lett. B **181**, 157 (1986).

[18] R. H. Dalitz, G. R. Goldstein, Phys. Rev. D **45**, 1531 (1992); M. Jezabek and J. H. Kühn, Phys. Rev. D **48**, 1910 (1993).

[19] M. Beneke *et al.*, In *Geneva 1999, Standard model physics (and more) at the LHC*, 419-529 [hep-ph/0003033].

[20] W. Bernreuther, J. Phys. G **35**, 083001 (2008).

[21] T. Aaltonen *et al.* [CDF Collaboration], Phys. Rev. Lett. **105**, 232003 (2010).

[22] V. M. Abazov *et al.* [D0 Collaboration], Phys. Rev. Lett. **106**, 022001 (2011).

[23] V.M. Abazov *et al.* [D0 Collaboration], Phys. Rev. D **85**, 091104 (2012).

[24] J. H. Kühn, Nucl. Phys. B **237** (1984) 77.

[25] V. D. Barger, J. Ohnemus and R. J. Phillips, Int. J. Mod. Phys. A **4**, 617 (1989).

[26] G. L. Kane, G. A. Ladinsky and C. P. Yuan, Phys. Rev. D **45**, 124 (1992).

[27] T. Arens and L. M. Sehgal, Phys. Lett. B **302**, 501 (1993).

[28] G. Mahlon and S. J. Parke, Phys. Rev. D **53**, 4886 (1996).

[29] T. Stelzer and S. Willenbrock, Phys. Lett. B **374**, 169 (1996).

[30] A. Brandenburg, Phys. Lett. B **388**, 626 (1996).

[31] D. Chang, S. -C. Lee and A. Sumarokov, Phys. Rev. Lett. **77**, 1218 (1996).

[32] W. Bernreuther, A. Brandenburg and P. Uwer, Phys. Lett. B **368**, 153 (1996).

[33] W. G. Dharmaratna and G. R. Goldstein, Phys. Rev. D **53**, 1073 (1996).

[34] G. Mahlon and S. J. Parke, Phys. Lett. B **411**, 173 (1997).

[35] W. Bernreuther, A. Brandenburg, Z. G. Si and P. Uwer, Phys. Rev. Lett. **87**, 242002 (2001).

[36] W. Bernreuther, A. Brandenburg, Z. G. Si and P. Uwer, Nucl. Phys. B **690**, 81 (2004).

[37] P. Uwer, Phys. Lett. B **609**, 271 (2005).

[38] C. A. Nelson *et al.*, Eur. Phys. J. C **45**, 121 (2006).

[39] R. M. Godbole, S. D. Rindani and R. K. Singh, J. High Energy Phys. 12, 021 (2006).

[40] W. Bernreuther, J. Phys. G **35**, 083001 (2008).

[41] G. Mahlon and S. J. Parke, Phys. Rev. D **81**, 074024 (2010).

[42] W. Bernreuther and Z. G. Si, Nucl. Phys. B **837**, 90 (2010).

[43] W. Bernreuther and Z. G. Si, Phys. Lett. B **725**, 115 (2013).

[44] T. Aaltonen *et al.* [CDF Collaboration], Phys. Rev. D **83**, 031104 (2011).

[45] V. M. Abazov *et al.* [D0 Collaboration], Phys. Lett. B **702**, 16 (2011).

[46] V. M. Abazov *et al.* [D0 Collaboration], Phys. Rev. Lett. **107**, 032001 (2011).

[47] V. M. Abazov *et al.* [D0 Collaboration], Phys. Rev. D **84**, 012008 (2011).

[48] ATLAS Collaboration, Phys. Rev. Lett. **108**, 212001 (2012).

[49] ATLAS Collaboration, arXiv:1407.4314 [hep-ex].

[50] CMS Collaboration, Phys. Rev. Lett. **112**, 182001 (2014).

[51] B. de Carlos and J. A. Casas, Phys. Lett. B **309**, 320 (1993).

[52] R. Barbieri and G. F. Giudice, Nucl. Phys. B **306**, 63 (1988).

[53] P. Fayet, Phys. Lett. B **64**, 159 (1976).

[54] P. Fayet, Phys. Lett. B **69**, 489 (1977).

[55] G. R. Farrar and P. Fayet, Phys. Lett. B **76**, 575 (1978).

[56] P. Fayet, Phys. Lett. B **84**, 416 (1979).

[57] S. Dimopoulos and H. Georgi, Nucl. Phys. B **193**, 150 (1981).

[58] CMS Collaboration, Eur. Phys. J. C **73**, 2677 (2013).

[59] ATLAS Collaboration, Phys. Rev. Lett. **109**, 211802 (2012).

[60] ATLAS Collaboration, Phys. Rev. Lett. **109**, 211803 (2012).

[61] ATLAS Collaboration, JHEP **1211**, 094 (2012).

[62] ATLAS Collaboration, arXiv:1407.0583 [hep-ex].

[63] ATLAS Collaboration, arXiv:1406.1122 [hep-ex].

[64] ATLAS Collaboration, JHEP **1406**, 124 (2014).

[65] ATLAS Collaboration, arXiv:1406.5375 [hep-ex].

[66] ATLAS Collaboration, J. Inst. **3**, S08003 (2008).

[67] GEANT4 Collaboration, S. Agostinelli *et al.*, Nucl. Instrum. Meth. A **506**, 250 (2003).

[68] ATLAS Collaboration, Eur. Phys. J. C **70** 823 (2010).

[69] S. Frixione and B. R. Webber, JHEP **06**, 029 (2002).

[70] S. Frixione, P. Nason and B. R. Webber, JHEP **0308**, 007 (2003).

[71] G. Corcella *et al.*, JHEP **01**, 010 (2001).

[72] H-L. Lai *et al.*, Phys. Rev. D **82**, 074024 (2010).

[73] M. Cacciari *et al.*, Phys. Lett. B **710**, 612 (2012).

[74] M. Beneke, P. Falgari, S. Klein and C. Schwinn, Nucl. Phys. B **855**, 695 (2012).

[75] P. Bärnreuther, M. Czakon and A. Mitov, Phys. Rev. Lett. **109**, 132001 (2012).

[76] M. Czakon and A. Mitov, JHEP **1212**, 054 (2012).

[77] M. Czakon and A. Mitov, JHEP **1301**, 080 (2013).

[78] M. Czakon, P. Fiedler and A. Mitov, Phys. Rev. Lett. **110**, 252004 (2013).

[79] M. Czakon and A. Mitov, Comput. Phys. Commun. **185**, 2930 (2014).

[80] M. Botje *et al.*, arXiv:1101.0538 [hep-ph].

[81] A. D. Martin, W. J. Stirling, R. S. Thorne and G. Watt, Eur. Phys. J. C **63**, 189 (2009).

[82] A. D. Martin, W. J. Stirling, R. S. Thorne and G. Watt, Eur. Phys. J. C **64**, 653 (2009).

[83] H. L. Lai *et al.*, Phys. Rev. D **82**, 074024 (2010).

[84] J. Gao *et al.*, Phys. Rev. D **89**, 033009 (2014).

[85] R. D. Ball *et al.*, Nucl. Phys. B **867**, 244 (2013).

[86] J. Alwall, M. Herquet, F. Maltoni, O. Mattelaer and T. Stelzer, JHEP **1106**, 128 (2011).

[87] T. Sjostrand, S. Mrenna and P. Skands, JHEP **0605**, 026 (2006).

[88] M. L. Mangano *et al.*, JHEP **0307**, 001 (2003).

[89] P. M.Nadolsky *et al.*, Phys. Rev. D **78**, 013004 (2008).

[90] R. Hamberg, W. L. van Neerven and T. Matsuura, Nucl. Phys. **B 359**, 343 (1991). [Erratum-ibid. **B 644**, 403 (2002)].

[91] J. Butterworth, J. Forshaw and M. Seymour, Z. Phys. C **72**, 637 (1996).

[92] M. L. Mangano *et al.*, Nucl. Phys. B **632**, 343 (2002).

[93] P. Nason, JHEP **0411**, 040 (2004).

[94] S. Frixione, P. Nason and C. Oleari, JHEP **0711**, 070 (2007).

[95] S. Alioli, P. Nason, C. Oleari and E. Re, JHEP **1006**, 043 (2010).

[96] E. Re, Eur. Phys. J. C **71**, 1547 (2011).

[97] N. Kidonakis, Phys. Rev. D **82**, 054018 (2010).

[98] T. Gleisberg *et al.*, JHEP **0902**, 007 (2009).

[99] J.M. Campbell and R.K. Ellis, Phys. Rev. D **60**, 113006 (1999).

[100] ATLAS Collaboration, Eur. Phys. J. C **71**, 1577 (2011).

[101] ATLAS Collaboration, JHEP **1205**, 059 (2012).

[102] M. Bahr *et al.*, Eur. Phys. J. C **58**, 639 (2008).

[103] W. Beenakker *et al.*, Nucl. Phys. B **515**, 3 (1998); W. Beenakker *et al.*, JHEP **1008**, 098 (2010); W. Beenakker *et al.*, Int. J. Mod. Phys. A **26**, 2637 (2011).

[104] ATLAS Collaboration, Eur. Phys. J. C **74**, 2941 (2014).

[105] ATLAS Collaboration, Eur. Phys. J. C **74**, 3034 (2014).

[106] ATLAS Collaboration, Eur. Phys. J. C **73**, 2304 (2013).

[107] M. Cacciari and G. P. Salam, Phys. Lett. B **641**, 57 (2006).

[108] M. Cacciari, G. P. Salam and G. Soyez, JHEP **0804**, 063 (2008).

[109] M. Cacciari, G. P. Salam and G. Soyez, Eur. Phys. J. C **72** (2012) 1896.

[110] ATLAS Collaboration, *Commissioning of the ATLAS high-performance b-tagging algorithms in the 7 TeV collision data*, ATLAS-CONF-2011-102, `http://cdsweb.cern.ch/record/1369219`.

[111] ATLAS Collaboration, *Measurement of the b-tag efficiency in a sample of jets containing muons with* 5 fb^{-1} *of data from the ATLAS detector*, ATLAS-CONF-2012-043, `http://cdsweb.cern.ch/record/1435197`.

[112] ATLAS Collaboration, Eur. Phys. J. C **72**, 1844 (2012).

[113] N. Reid and D.A.S. Fraser, in Proceedings of PHYSTAT 2003, edited by L. Lyons, R.P. Mount, and R. Reitmeyer, (SLAC, Stanford, 2003), p. 265.

[114] ATLAS Collaboration, Eur. Phys. J. C **72**, 2043 (2012).

[115] C. D. White, S. Frixione, E. Laenen and F. Maltoni, JHEP **0911** (2009) 074.

[116] G. Cowen *et al.*, Eur. Phys. J. C **71**, 1554 (2011).

[117] A. L. Read, J. Phys. G **28**, 2693 (2002).

[118] M. Kramer *et al.*, arXiv:1206.2892 [hep-ph].